

# ON-DEVICE COLLABORATIVE LANGUAGE MODELING VIA A MIXTURE OF GENERALISTS AND SPECIALISTS

Dongyang Fan\*, Bettina Messmer\*, Martin Jaggi

EPFL, Lausanne, Switzerland

{firstname.lastname}@epfl.ch

## ABSTRACT

We target on-device collaborative fine-tuning of Large Language Models (LLMs) by adapting a Mixture of Experts (MoE) architecture, where experts are Low-Rank Adaptation (LoRA) modules. In conventional MoE approaches, experts develop into specialists throughout training. In contrast, we propose a novel Collaborative learning approach via a **M**ixture of **G**eneralists and **S**pecialists (CoMiGS). Diversifying into the two roles is achieved by aggregating certain experts globally while keeping others localized to specialize in user-specific datasets. Central to our work is a learnable routing network that routes at a token level, balancing collaboration and personalization at the finest granularity. Our method consistently demonstrates superior performance in scenarios with high data heterogeneity across various datasets. By design, our approach accommodates varying computational resource constraints among users as shown in different numbers of LoRA experts. We further showcase that low-resourced users can benefit from high-resourced users with high data quantity.

## 1 INTRODUCTION

Large Language Models (LLMs) have been showing great success serving as foundation models, evidenced by their capability to understand a wide range of tasks. Their applicability and personalized adaptation to end users can further be enhanced by fine-tuning on device. On-device fine-tuning of LLMs poses new challenges such as restricted and varying computational resources, scarce and heterogenous local data, and privacy concerns related to data sharing. As a solution, we study personalized collaborative on-device fine-tuning of LLMs in this work.

A parameter-efficient method for performing LLM fine-tuning is through Low-Rank Adaptors (LoRA, Hu et al. (2021)), where model updates ( $\Delta \mathbf{W} \in \mathbb{R}^{m \times n}$ ) are approximated by the multiplication of two low-rank matrices  $\mathbf{A} \in \mathbb{R}^{m \times r}$  and  $\mathbf{B} \in \mathbb{R}^{r \times n}$  ( $r \ll m, n$ ). However, when system heterogeneity arises—meaning users are equipped with different-sized LoRA modules—collaboration through simple model parameter aggregation becomes unfeasible. Previous works have proposed various techniques for aggregating LoRA modules of different ranks (Cho et al., 2023; Bai et al., 2024). In this work, we address system heterogeneity by allowing users to have varying numbers of LoRA modules. That is, high-resourced users are equipped with a larger number of LoRA modules locally.

The aggregation of LoRA modules within a user can be done through a Mixture-of-Experts (MoE) fashion, where each LoRA module is regarded as an expert, as in Wu et al. (2024); Zadouri et al. (2024). Typically, a Multi-layer Perceptron (MLP) routing network dynamically assigns input units to each expert, and the expert scores serve as aggregation weights to combine expert outputs. Routing is often done at the token level, a design choice proven to bring optimal performances (Jiang et al., 2024; Fan et al., 2024b). Tokens within an input sequence are directed to various experts based on the routing mechanism. Since the routing and expert networks are jointly trained, the diversification of experts occurs naturally. It is observed that different experts develop distinct context-independent specializations in syntax and locality. (Jiang et al., 2024; Xue et al., 2024). We call these experts *specialists*. While specialist experts show promising results, can the performances be further advanced by introducing some experts with more general knowledge (*generalists*)?

The modular nature of MoEs facilitates the coexistence of generalists and specialists in a collaborative learning setup. It allows for the separation of certain experts, whose parameters can be aggregated

---

across users (*generalists*), while other experts remain localized to specialize in user-specific data (*specialists*). Presumably, generalists are of importance, particularly in language modeling. End users, such as mobile device users, may have unique topics or language patterns but frequently share common tokens in their vocabularies (see Figure 5). Jointly learning these shared tokens should be more efficient than each user learning them alone.

Additionally, MoE architecture can deal with system heterogeneity nicely, allowing users to have varying numbers of specialists as long as the number of generalist experts remains consistent for aggregation. This enables high-resourced users to leverage more experts for their local data, while low-resourced users still benefit from shared expertise.

Balancing personalization and collaboration is a challenging task in collaborative learning. Typically, the challenge is addressed at a client level, where a pairwise collaboration graph is inferred from gradient or prediction similarity across users (Fan et al., 2024a; Wagner et al., 2024). We take a novel approach by addressing it at a token level. Our approach leverages the powerful routing mechanism of MoEs, where the routing results are used to weigh generalist and specialist experts for each input token. The finest-grained approach should offer the most tailored solution to the end users.

In summary, our contributions are as follows:

- We propose a novel approach (CoMiGS) for on-device personalized collaborative fine-tuning of LLMs, by introducing a mixture of generalist and specialist LoRA experts. The approach balances personalization and collaboration at the finest granularity.
- Our collaborative framework effectively addresses both *system heterogeneity*, with respect to varying local model architectures, and *data heterogeneity*, concerning diverse local data distributions across users, making it the first model to accomplish both.
- Our framework separates resource heterogeneity from data quantity. Users with larger datasets benefit from a bigger model, while high-resourced users with smaller datasets are less prone to overfitting.

## 2 RELATED WORK

**Collaborative Learning for LLMs.** Recently, researchers have been investigating the application of Federated Learning in language tasks. Due to the substantial number of model parameters in LLMs, the research has largely targeted the stages following pre-training, often utilizing parameter-efficient techniques such as adapters. Mohtashami et al. (2023) explored a teacher-student social learning framework to aggregate private-sensitive instructions. Zhang et al. (2023) directly applied FedAvg (McMahan et al., 2017) to aggregate LoRA parameters during instruction tuning, and reported increased performance in downstream tasks. Following that, there are various works focusing on addressing system heterogeneity where users are equipped with different LoRA ranks. HetLoRA (Cho et al., 2023) and FlexLoRA (Bai et al., 2024) provide different ways of aggregating and distributing LoRA modules of heterogeneous ranks. However, these approaches are not designed to cope with heterogeneous data on device. In contrast, Sun et al. (2024) found better performances with respect to heterogeneous data can be achieved through freezing LoRA A matrices at initialization; Wagner et al. (2024) proposed personalized solutions that can sufficiently tackle data heterogeneity, through three different collaborator selection mechanisms. Yet for both works, the users must be equipped with the same model architecture. Unlike previous works, our framework deals with both model heterogeneity and data heterogeneity. Moreover, our method offers personalized solutions at a token level, as opposed to the client-level approach in Wagner et al. (2024).

**Mixture of Generalist and Specialist Experts.** Gaspar & Seddon (2022) introduced a fusion of global and local experts for activity prediction based on molecular structures. Each local expert is tailored to a specific chemical series of interest using loss masking, while a global expert is trained across all series. Simultaneously, a routing network learns to assign soft merging scores. This approach yielded superior empirical results compared to single experts. Dai et al. (2024) developed DeepSeekMoE by deterministically assigning every token to “shared” experts, whereas “routed” experts are assigned tokens based on a learnable router. DeepSeekMoE is able to approach the upper bound performance for MoE models. For both works, the notion of shared/global is with respect to input samples, i.e. a shared/global expert should see all input samples. In a collaborative

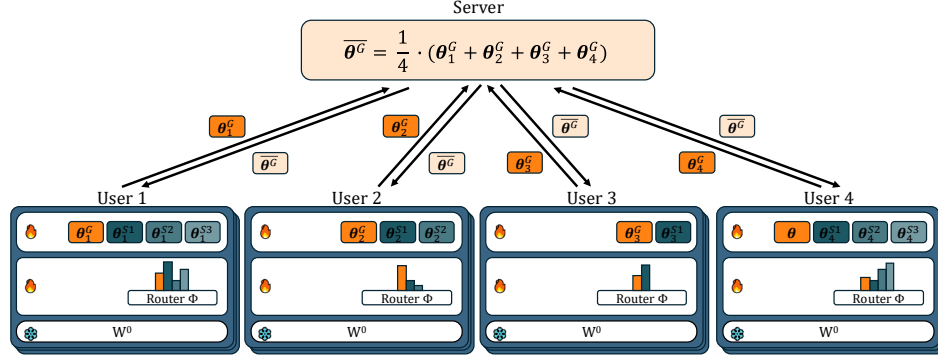


Figure 1: Diagram of our proposed method illustrated with a 4-client setup, with a dark blue frame denoting a block. Within each block, generalist experts ( $\{\theta_1^G, \theta_2^G, \theta_3^G, \theta_4^G\}$ ) are aggregated across users, and specialist experts ( $\{\theta_1^{S1}, \theta_2^{S1}, \theta_3^{S1}, \theta_4^{S1}\}$ ) are kept local. Router and expert parameters are updated iteratively using local validation and training datasets.

setup, Yi et al. (2024) proposed pFedMoE, where each user has a shared homogeneous small feature extractor, a localized heterogeneous feature extractor, and a localized routing network. The three components are updated simultaneously in an end-to-end manner. Such an architecture demonstrates superior performance in the vision domain. Our work extends the idea of pFedMoE to the language domain, and re-formulates it as a bilevel optimization problem, focusing on the central role of the data-dependent routing mechanism.

### 3 METHOD

Aiming to achieve better personalized performance for each user, we propose leveraging collective knowledge while maintaining specialized expertise within each user through a mixture of generalist and specialist experts. As a solution, we introduce a multi-round, gradient-based algorithm based on the following key insights: (1) generalist models emerge through the aggregation of weights during communication rounds, and (2) expert and routing parameters are updated alternately, guided by two distinct and disentangled loss functions. We formalize our problem setup and solution as follows:

#### 3.1 NOTIONS AND PROBLEM SETUP

Each user has a training set  $\mathbf{X}_i^{\text{train}}$ , a small validation set  $\mathbf{X}_i^{\text{valid}}$  and a test set  $\mathbf{X}_i^{\text{test}}$ , and the task is next token prediction. The validation set  $\mathbf{X}_i^{\text{valid}}$  and the test set  $\mathbf{X}_i^{\text{test}}$  are sampled from the same distribution  $\mathcal{P}_i^{\text{target}}$  (note this is a fuzzy concept in the language domain, by the same distribution we mean from the same topic/category). The training set,  $\mathbf{X}_i^{\text{train}}$ , can be sampled from a different distribution than  $\mathcal{P}_i^{\text{target}}$ . This is to address scenarios where distribution shifts may occur over time, such as changes in topics reflected in the typing data of mobile phone users.

As illustrated in Figure 1, there are two sets of model parameters within each user: expert parameters, denoted as  $\Theta = \theta^G \cup \{\theta_i^S\}$ , where  $\theta^G$  is shared across the users and  $\{\theta_i^S\}$  are user-specific specialist parameters; and routing parameters, denoted as  $\Phi = \{\phi_i\}$ .  $i \in [0, N)$  is the user index. The  $\theta$ s are a union of LoRA A and B matrices. Our ultimate goal is to optimize the average performance of users, following the averaged personalized learning objectives on user-specific targets:

$$\min_{\Theta, \Phi} \frac{1}{N} \sum_i \mathcal{L}(f(\mathbf{X}_i^{\text{test}}; \theta^G, \theta_i^S, \phi_i), \mathbf{X}_i^{\text{test}}) \quad (1)$$

where  $\mathcal{L}$  is the language modeling loss. Note we write  $\mathbf{X}_i^{\text{test}}$  as the label here, as this is a self-supervised task. Labels are simply shifted inputs.

#### 3.2 OUR APPROACH

Since the objective in (1) is unattainable due to the unavailability of test loss during training, we approximate it using validation loss. We further reformulate our proxy objective as a bi-level

---

**Algorithm 1** Pseudo code of our proposed algorithm

---

**Input:** Expert parameters  $\{\theta_{i,0}^G, \theta_{i,0}^S\}$ , routing parameters  $\{\phi_{i,0}\}$ . Local training data and validation data  $\{\mathbf{X}_i^{\text{train}}, \mathbf{X}_i^{\text{valid}}\}$ ,  $i \in [0, N)$ . Communication round  $T$  and routing update period  $\tau$ . Load balancing weight  $\lambda$ .

**for**  $t = 1, \dots, T$  **do**

Server aggregates generalist parameters:  $\theta_{t-1}^G = \frac{1}{N} \sum_i \theta_{i,t-1}^G$

**for**  $i \in [0, N)$  **do**

Users download aggregated generalist weights and

prepare model parameters for training  $\{\theta_{t-1}^G, \theta_{i,t-1}^S, \phi_{i,t-1}\}$

Do gradient steps on  $(\theta_{t-1}^G, \theta_{i,t-1}^S)$  towards minimizing (2) and get  $(\theta_{i,t}^G, \theta_{i,t}^S)$

$$\min_{\theta_i^G, \theta_i^S} \mathcal{L}(f(\mathbf{X}_i^{\text{train}}; \theta_i^G, \theta_i^S, \phi_{i,t-1}), \mathbf{X}_i^{\text{train}}) + \lambda \cdot \mathcal{L}_i^{\text{LB}}(\mathbf{X}_i^{\text{train}}; \theta_i^G, \theta_i^S, \phi_{i,t-1}) \quad (2)$$

**if**  $t \% \tau = 0$  **then**

Do gradient steps on  $\phi_{i,t-1}$  towards minimizing (3) and get  $\phi_{i,t}$

$$\min_{\phi_i} \mathcal{L}(f(\mathbf{X}_i^{\text{valid}}; \theta_{i,t}^G, \theta_{i,t}^S, \phi_i), \mathbf{X}_i^{\text{valid}}) + \lambda \cdot \mathcal{L}_i^{\text{LB}}(\mathbf{X}_i^{\text{valid}}; \theta_{i,t}^G, \theta_{i,t}^S, \phi_i) \quad (3)$$

**end if**

**end for**

Each device  $i \in [0, N)$  sends generalist weights  $\theta_{i,t}^G$  to the server

**end for**

**Return:** Expert parameters  $\{\theta_{i,T}^G, \theta_{i,T}^S\}$  and routing parameters  $\{\phi_{i,T}\}$

---

optimization problem, as presented in (4). The routing parameters  $\Phi = \{\phi_i\}$  are updated based on the validation loss, which reflects the target distribution (outer optimization), while the expert parameters  $\Theta = \theta^G \cup \{\theta_i^S\}$  are updated using the training loss (inner optimization). This formulation arises from the idea that expert knowledge can be effectively developed from the large training sets, while how to combine that knowledge should remain target-specific.

$$\begin{aligned} \min_{\Phi} \sum_i \mathcal{L}(f(\mathbf{X}_i^{\text{valid}}; \Theta^*(\Phi), \phi_i), \mathbf{X}_i^{\text{valid}}) \\ \text{s.t. } \Theta^*(\Phi) \in \arg \min_{\Theta} \sum_i \mathcal{L}(f(\mathbf{X}_i^{\text{train}}; \theta^G, \theta_i^S, \phi_i), \mathbf{X}_i^{\text{train}}) \end{aligned} \quad (4)$$

To solve (4), we use a multi-round gradient-based algorithm as shown in Alg.1, where only generalist parameters are shared and aggregated, and specialist parameters and router weights are updated locally. While the scheme requires a server, it can alternatively be implemented in a serverless all2all fashion, which requires  $N$  times more communication overhead and we do not further pursue this here.

### 3.3 ALGORITHMIC HIGHLIGHTS

**Alternating Update of  $\Theta$  and  $\Phi$ :** Alternating update of two sets of parameters is a standard way to solve bi-level optimization problems. In between two communication rounds, we perform alternating updates of expert and routing parameters using local training and validation sets separately. The updates optimize the objectives given in (2) and (3) respectively. Since the updates of  $\Theta$  and  $\Phi$  are disentangled, they do not need to be updated at the same frequency. The routing parameters are smaller in size and thus can be updated less frequently. An empirical evidence is provided in Fig. 9.

When updating expert parameters, we include an additional load-balancing term as in Fedus et al. (2022), which is standard in MoE implementation and encourages even distribution of token assignments to experts. A discussion over the load balancing term is included in Appendix C.3. It is observed that a load-balancing term can improve test performance compared to not having one. However, directing more tokens to the generalists has no noticeable effect.



**Update of  $\theta^G$  and  $\theta_i^S$ :** The update of generalist parameters  $\theta^G$  follows a standard FedAvg scheme, through aggregating model parameters. Specifically, we simultaneously update both  $\theta^G$  and  $\theta_i^S$  by optimizing equation (2), which results in  $\theta_i^G$  and  $\theta_i^S$ . A parameter aggregation is then performed on the user-specific  $\theta_i^G$  via a trusted server to establish a shared  $\theta_G$  across all users. In the next round, each user replaces their  $\theta_i^G$  with the global  $\theta_G$ , while their  $\theta_i^S$  remains locally updated.

## 4 EXPERIMENTS

### 4.1 SETUP

#### 4.1.1 DATASETS

We selected three diverse distributed datasets to showcase the efficacy of our proposed algorithm:

- i) *Multilingual Wikipedia*: This dataset constitutes Wikipedia articles in four languages: German, Dutch, French, and Italian. We take German, French and Italian from Wikimedia-Foundation, and Dutch from Guo et al. (2020);
- ii) *SlimPajama*: we pick the following four categories – StackExchange, Github, ArXiv, Book from Soboleva et al. (2023);
- iii) *AG News*: This dataset covers News from categories of World, Sports, Business, and Sci/Tech (Zhang et al., 2016).

Opting for the most challenging scenario, each user is assigned a unique category, as shown in Figure 2, where users can have varying data quantities. Given our emphasis on next token prediction, we anticipate shared predictions among users while maintaining category-specific distinctions. For details of our user data splits, please refer to Appendix B.

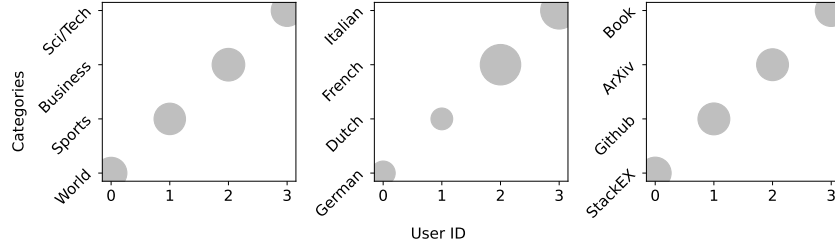


Figure 2: The data splits across users, with bubble size denoting the relative size of the local dataset.

#### 4.1.2 EXPERIMENTAL DETAILS

Our base model is the GPT2 model with 124M parameters<sup>1</sup>, which is suitable for on-device deployment. We incorporate LoRA modules into every linear layer, including MLP and Self-Attention Layers, following the recommendations of Fomenko et al. (2024), specifically in the `[attn.c_attn, attn.c_proj, mlp.c_fc, mlp.c_proj]` layers. A routing mechanism is exclusively implemented atop MLP layers. This means that each attention layer has only one LoRA expert applied to it, which is always aggregated during synchronization. The number of LoRA experts in MLP blocks depends on the local resource abundance.

We use a constant learning rate of  $2 \times 10^{-3}$  for updating routing parameters and a  $2 \times 10^{-3}$  learning rate with a one-cycle cosine schedule for expert parameters during fine-tuning. The LoRA rank  $r$  is set to 8 unless otherwise specified, with LoRA alpha  $\alpha$  set to 16, following the common practice of setting alpha to twice the rank (Raschka, 2023). A load balancing weight 0.01 is always applied. For more experimental details, we refer readers to Appendix B.

### 4.2 DATA-DRIVEN SELECTION: GENERALIST VS. SPECIALIST

We start by equipping users with the same model architecture locally, to study the powerfulness of our routing mechanism. In our setup every user has two LoRA experts locally. We compare our one

<sup>1</sup>We adopt the codes from <https://github.com/karpathy/nanoGPT> and <https://github.com/danielgrittner/nanoGPT-LoRA>

generalist one specialist (CoMiGS-1G1S) method to the following baselines. In order to match the trainable parameter count of our method, we use 2 times LoRA modules within each user.

- i) • **Pretrained:** A pretrained GPT-2 model using weights from OpenAI.
- **Centralized:** A single model trained using data from all users. (Note this method is an unrealistic baseline as data cannot leave the devices due to privacy concerns.)
- ii) • **Local:** Training individually using only local data without collaboration.
- **FedAvg:** Aggregating LoRA parameters across users using uniform weights, which is equivalent to applying FedAvg (McMahan et al., 2017).
- **PCL:** Aggregating LoRA parameters using a client-level collaboration graph. The graph is updated using validation performances. (Strategy 2 in Wagner et al. (2024)).
- iii) • **CoMiGS-2S:** Both of the LoRA experts are specialists, that is, their weights are never shared and aggregated. The routing parameters are updated using a separate validation set like CoMiGS-1G1S.
- **CoMiGS-2G:** Both of the LoRA experts are generalists, that is, their weights are always shared and aggregated. The routing parameters are updated using a separate validation set like CoMiGS-1G1S.

The comparison between ii) and iii) serves to illustrate the role of our routing mechanism, while the comparison between our CoMiGS-1G1S and iii) demonstrates the benefit of the coexistence of both specialists and generalists. To show the wide applicability of our method, we focus on the following two tasks:

**In-Domain Tasks.** Within each user, we create validation/test datasets from the same domain as the training sets. Here we address the following two scenarios: i) diversity in language usage across users (Multilingual Wikipedia) ; ii) diversity in topic coverage across users (SlimPajama).

**Out-of-Domain Tasks.** Within each user, we create validation/test datasets from a different distribution than in the training sets. During training, each user has one News category from AG News. However, the validation and test sets for each user are a homogeneous mixture of all categories. This is to account for possible topic changes within users.

#### 4.2.1 RESULT ANALYSIS

The comparison between our method and the baseline methods is summarized in Table 1. We provide an extension of baseline comparison in Appendix C.1.

**Effectiveness of our routing mechanism:** Depending on the dataset, either CoMiGS-2G or CoMiGS-2S achieves the highest performance. The key distinction compared to Local or FedAvg is the existence of a layer-wise router, which weighs the two generalists or two specialists for each token, as opposed to assigning equal weights. This highlights the effectiveness of our learned routing mechanism.

**Token-level vs. client-level collaborative decisions:** Compared to the state-of-the-art baseline, PCL, as proposed by Wagner et al. (2024), our method demonstrates a clear performance improvement. PCL assigns a pairwise collaboration weight between users by evaluating how well user  $i$ ’s model performs on user  $j$ ’s validation set. On the two in-domain tasks, PCL exhibits performance similar to Local, where the resulting collaboration matrices are nearly identity matrices, thereby limiting effective collaboration between users. Our method, in contrast, decides the collaboration pattern based on each input token, and thus can harness the collective power more effectively.

**The impact of co-existence of generalists and specialists:** The performances of CoMiGS-2G and CoMiGS-2S are not consistent across the different scenarios, while our CoMiGS-1G1S can always closely track the best-performing model, which is clearly shown in Figure 3. Depending on the task type, generalists and specialists alone may not be sufficient. A balanced combination of personalization and collaboration is required, and our approach achieves this balance effectively.

#### 4.2.2 ROUTING ANALYSIS

**Layer-wise analysis:** Figure 4 illustrates the evolution of averaged layer-wise routing scores for the generalist and specialist experts. As training progresses, specialists gradually take over the role

|                      | AG News   | Multilingual                                      | SlimPajama  |
|----------------------|---|---|---|
| <i>Pretrained</i>    | 90.65   | 156.12  | 37.19   |
| <i>Centralized</i>   | 28.19 (0.52) <span style="color: black;">█</span> | 55.41 (0.12) <span style="color: black;">█</span> | 19.53 (0.14) <span style="color: black;">█</span> |
| <i>Local</i>         | 41.50 (0.05) <span style="color: black;">█</span> | 55.49 (0.64) <span style="color: black;">█</span> | 27.31 (0.17) <span style="color: black;">█</span> |
| <i>FedAvg</i>        | 32.24 (0.05) <span style="color: black;">█</span> | 56.90 (0.16) <span style="color: black;">█</span> | 23.30 (0.17) <span style="color: black;">█</span> |
| <i>PCL</i>           | 32.11 (0.04) <span style="color: black;">█</span> | 54.02 (0.19) <span style="color: black;">█</span> | 27.12 (0.33) <span style="color: black;">█</span> |
| <i>CoMiGS - 2S</i>   | 35.81 (0.13) <span style="color: black;">█</span> | 46.36 (0.16) <span style="color: green;">█</span> | 22.51 (0.08) <span style="color: black;">█</span> |
| <i>CoMiGS - 2G</i>   | 31.18 (0.05) <span style="color: green;">█</span> | 58.31 (0.17) <span style="color: black;">█</span> | 21.36 (0.01) <span style="color: green;">█</span> |
| <i>CoMiGS - 1G1S</i> | 33.53 (0.03) <span style="color: red;">█</span>   | 47.19 (0.10) <span style="color: red;">█</span>   | 21.79 (0.04) <span style="color: red;">█</span>   |

Table 1: Mean test perplexity over the users with homogeneous models, averaged across 3 seeds. Mean (std) with a rank locator for the mean (the lower the better). Green denotes the best performing methods and red denotes our method.

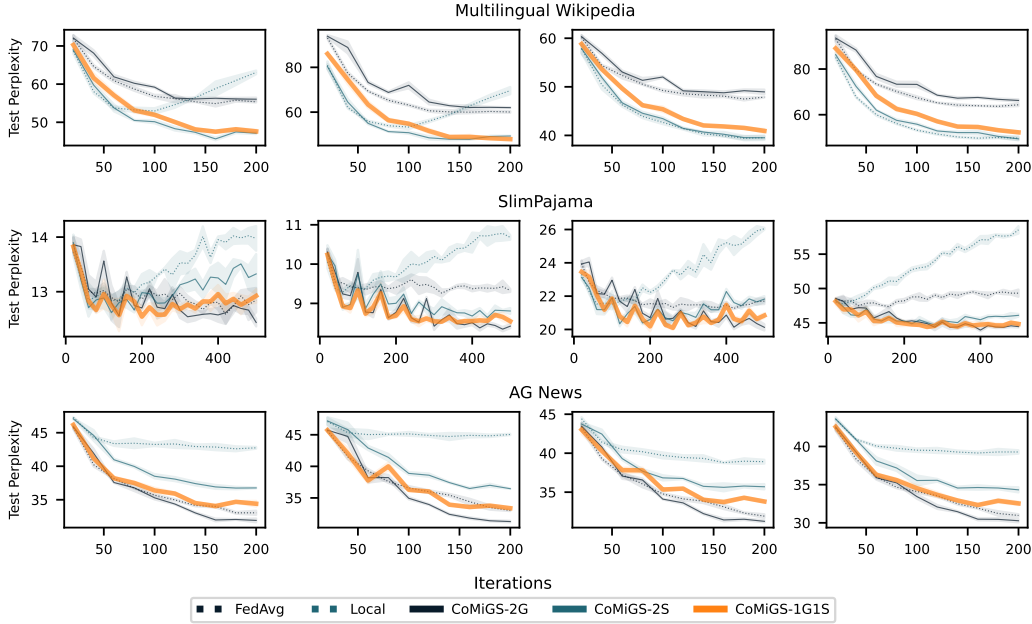


Figure 3: Test Perplexity during training for all the three datasets: our method closely follows the best performing method

of generalists across all layers. Notably, for out-of-domain tasks such as AG News, generalists play a more significant role early in training. By the end of training, the score distribution stabilizes, with generalists still contributing 30%-50% to next-token predictions, underscoring their importance in handling out-of-domain tasks. For in-domain tasks, more weight is shifted toward specialists. However, generalists still hold considerable importance, especially in datasets like SlimPajama, where some users are locally exposed to math or code-related texts, and generalists are needed to better process standard texts. Additionally, it is observed that deep layers have more skewed score distributions, while shallow layers weigh generalists and specialists more evenly.

**Token-wise analysis:** We further present a token-level routing result visualization on models fine-tuned with SlimPajama dataset in Figure 5: Users 0 and 1 are fine-tuned with very specific math and programming texts, and they tend to utilize the generalist more in the last layer. Function words ("and", "a", "on", "the" etc) are more routed to generalists, as expected. This can be seen in the top right panel of Figure 5. It is important to note that only the top choice is highlighted here. The abundance of blue does not imply that generalist experts play no role in predicting the next token. To see this, compared to when only specialists are present (CoMiGS-2S), our CoMiGS-1G1S gives more consistent results. More detailed token-wise routing result visualization including out-of-domain

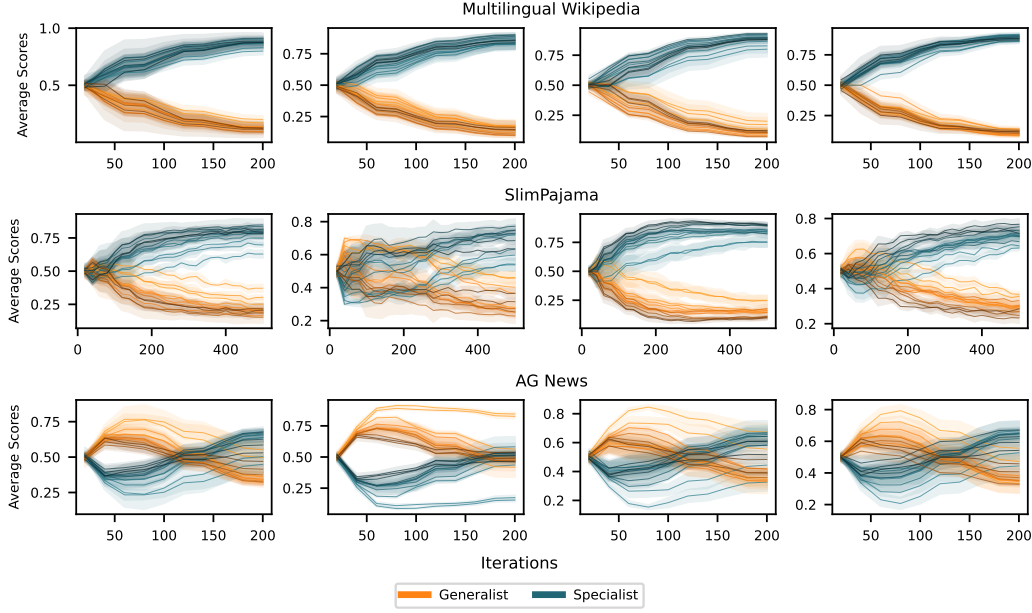


Figure 4: Expert Scores for the *generalist* expert and the *specialist* expert, averaged across all tokens and multiple batches for all datasets. Darker colors represent deeper layers.

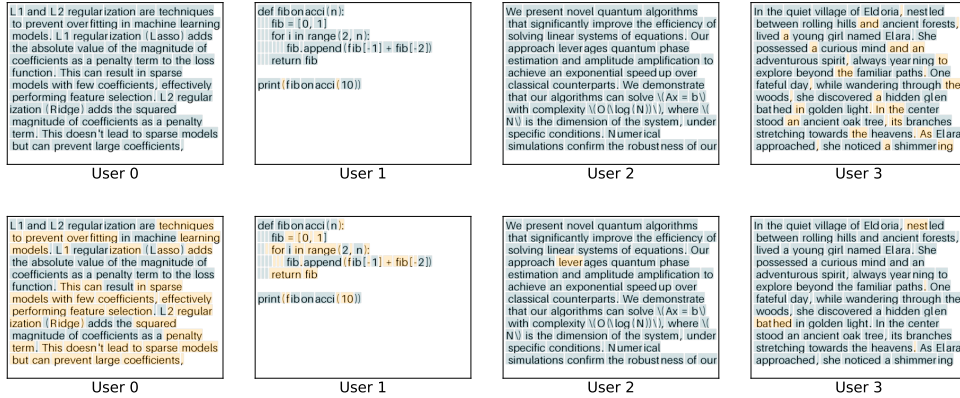


Figure 5: Visualization of in-domain token-level routing results for *IGIS* trained on SlimPajama. Tokens are colored with the Top1 expert choice at the first layer (top) and last layer (bottom). Orange denotes the generalist and blue denotes the specialist. Users 0-3 are trained with the categories StackExchange, GitHub, ArXiv, and Book respectively. Texts are generated by ChatGPT.

tasks can be seen in Appendix E. When dealing with out-of-domain texts, there is an increasing tendency to seek for generalists, as shown in the off-diagonal entries in Fig. 15.

### 4.3 ADAPTATION TO RESOURCE HETEROGENEITY

#### 4.3.1 BASELINE COMPARISON

In this section, our focus is to deal with system heterogeneity, where users can have different numbers of experts. We still keep one generalist expert, but the number of specialists can vary across the users (our method is denoted as CoMiGS-1GXS). It's important to note that the richness of computational resources doesn't always correlate with the complexity of local data. For instance, some users may have ample computational resources but local data in small quantities. In such cases, a crucial objective is to prevent overfitting due to redundant model-fitting abilities.

We compare our approach to two state-of-the-art baselines: `HetLoRA` from Cho et al. (2023) and `FlexLoRA` from Bai et al. (2024), both of which adapt LoRA ranks based on the resource capacity of each user. `HetLoRA` aggregates LoRA matrices  $A$  and  $B$  by zero-padding to the maximum rank and then distributes them back using rank truncation. In contrast, `FlexLoRA` first reconstructs model updates  $\Delta W$  and redistributes the aggregated updates using SVD. We compare our method to these baselines by matching the number of fine-tunable parameters, measured as both active and full parameters. For example, to match the full parameter count of 1GXS with (4, 2, 2, 2) LoRA experts (rank 8), LoRA modules of ranks (32, 16, 16, 16) would be required. With Top2 routing, to match the active parameter count, each user would need LoRA modules of rank 16.

Our results, shown in Table 2, are based on randomly assigning varying capabilities to users, independent of their local data size, as indicated by the number of LoRA modules per user. We find that our method outperforms the baseline methods most of the time, regardless of whether we match the full parameter count or the active parameter count. This advantage stems from the fact that both `HetLoRA` and `FlexLoRA` average model parameters across users without allocating parameters for local adaptations, focusing on building a strong generalist model. In contrast, our approach adaptively integrates both generalist and specialist knowledge, excelling in scenarios where specialized knowledge is crucial.

|                     | Ours         | HetLoRA      |              | FlexLoRA     |              |
|---------------------|--------------|--------------|--------------|--------------|--------------|
|                     |              | Active       | Full         | Active       | Full         |
| <b>AG News</b>      |              |              |              |              |              |
| (4,2,2,2)           | 33.66 (0.07) | 31.58 (0.14) | 31.95 (0.13) | 36.45 (0.06) | 36.49 (0.17) |
| (2,4,4,4)           | 34.22 (0.09) | 31.58 (0.14) | 32.52 (0.19) | 36.45 (0.06) | 36.40 (0.08) |
| <b>Multilingual</b> |              |              |              |              |              |
| (2,2,4,4)           | 46.48 (0.16) | 57.76 (0.10) | 58.60 (0.20) | 77.65 (0.20) | 77.85 (0.26) |
| (4,4,2,2)           | 47.24 (0.09) | 57.76 (0.10) | 59.14 (0.04) | 77.65 (0.20) | 76.29 (0.17) |
| <b>SlimPajama</b>   |              |              |              |              |              |
| (2,4,4,2)           | 22.10 (0.17) | 23.33 (0.10) | 23.15 (0.09) | 22.97 (0.11) | 22.99 (0.08) |
| (4,2,2,4)           | 22.28 (0.09) | 23.33 (0.10) | 23.17 (0.09) | 22.97 (0.11) | 22.99 (0.09) |

Table 2: Mean test perplexity (std) over users with heterogeneous models, averaged across 3 seeds, with **red** being the top1 method. For example, (4, 2, 2, 2) means in our 1GXS setup users have 4, 2, 2, and 2 experts, respectively, and in the two baselines, all users have rank 16 to match active parameter count, or ranks 32, 16, 16, and 16 to match full parameter count.

#### 4.3.2 ANALYSIS RELATED TO LOCAL DATA QUANTITIES

In this section, we further separate resource abundance from data quantity. Our approach is more robust to overfitting due to the regularizing effect of the generalist, while at the same time better fitting local data through the incorporation of specialist knowledge.

**More Specialists Help with Higher Data Quantity.** From Figure 3 we observe that the local data complexity for User 0 and User 1 is quite low: doing local model training with two times LoRA modules is prone to over-fitting. This is confirmed by low data quantity in both users in Figure 2. Instead, User 2 and User 3 benefit from longer local training. In the experiment shown in Figure 6 we validate that providing User 2 and User 3 more resources, by increasing the number of local experts to 4 and 8 (while still keeping top2 routing) indeed increases performance for both users.

**Generalists Help to Prevent Redundant Specialists from Over-Fitting.** In practice, users may not know their local data complexity, leading to a potential mismatch in resource allocation relative to data quantity. To simulate such scenarios, we allocate more experts to users with less data, specifically User 0 and User 1. Figure 7 demonstrates that our method is resilient to overfitting, even when fine-tuning twice or four times as many expert parameters.

**Specialists Can Benefit Generalists.** What if users can only support at most one expert? When those users participate in collaboration, in our setup they have to go with the generalist expert. We show that if we allocate more specialists to users with a higher local data quantity, the generalist knowledge can further be refined, as illustrated by the performance of User 0 and User 1 in Figure 8.

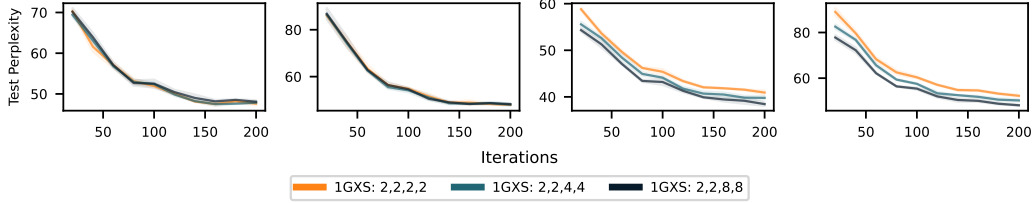


Figure 6: Test Perplexity during training for the multilingual setup. User 2 and User 3 have more data locally and thus benefit from having more experts. The numbers in the legend indicate the number of experts  $n_i$  within each user. Top-2 routing is performed.

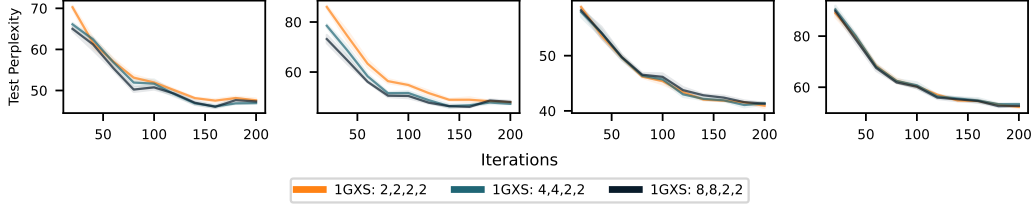


Figure 7: In the multilingual setup, Users 0 and 1 despite having high resources locally, do not overfit on their small-sized local data. Numbers in the legend denote the number of experts  $n_i$  within each user. Top2 routing is performed.

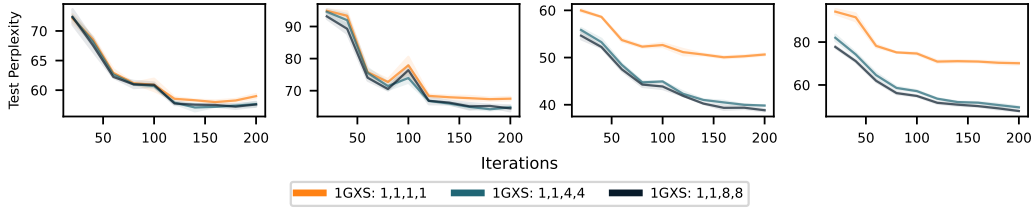


Figure 8: In the multilingual setup, Users 0 and 1, despite having only one expert locally, still benefit from other users having more experts, thereby enhancing the generalist’s performance. The numbers in the legend indicate the number of experts,  $n_i$ , within each user. Top-2 routing is applied when  $n_i \geq 2$ .

We provide an additional example of the impact of local data quantities in Appendix D using SlimPajama dataset. Similar conclusions can be drawn from our empirical results. However, there is a limit to how much generalists can help prevent overfitting when the local tasks are easy.

## 5 CONCLUSIONS AND FUTURE DIRECTIONS

Building on the Mixture of Experts (MoE) architecture, we propose a novel framework for on-device personalized collaborative fine-tuning of LLMs, which combines generalist and specialist experts. Our carefully designed routing mechanism ensures a balance between personalization and collaboration for each input token. This data-dependent approach consistently delivers strong performance across various datasets and task distributions.

Moreover, our framework adapts to varying local data sizes and computational resource constraints. High-resourced users can leverage larger datasets for enhanced performance while maintaining resilience against overfitting in scenarios with limited data.

An interesting future direction to explore is adopting our framework for collaborative instruction tuning of larger LLMs and evaluating its performance on downstream tasks. While our paper focused on a single generalist, it is possible to include multiple generalists, and their impact on performance remains to be seen. We hope our work paves the way for a new direction in on-device collaborative LLMs.

---

## REFERENCES

- Jiamu Bai, Daoyuan Chen, Bingchen Qian, Liuyi Yao, and Yaliang Li. Federated fine-tuning of large language models under heterogeneous language tasks and client resources. *arXiv preprint arXiv:2402.11505*, 2024.
- Yae Jee Cho, Luyang Liu, Zheng Xu, Aldi Fahrezi, Matt Barnes, and Gauri Joshi. Heterogeneous loRA for federated fine-tuning of on-device foundation models. In *International Workshop on Federated Learning in the Age of Foundation Models in Conjunction with NeurIPS 2023*, 2023. URL <https://openreview.net/forum?id=EmV9sGpZ7q>.
- Damai Dai, Chengqi Deng, Chenggang Zhao, R. X. Xu, Huazuo Gao, Deli Chen, Jiashi Li, Wangding Zeng, Xingkai Yu, Y. Wu, Zhenda Xie, Y. K. Li, Panpan Huang, Fuli Luo, Chong Ruan, Zhifang Sui, and Wenfeng Liang. Deepseekmoe: Towards ultimate expert specialization in mixture-of-experts language models, 2024.
- Dongyang Fan, Celestine Mender-Dünner, and Martin Jaggi. Collaborative learning via prediction consensus. *Advances in Neural Information Processing Systems*, 36, 2024a.
- Dongyang Fan, Bettina Messmer, and Martin Jaggi. TOWARDS AN EMPIRICAL UNDERSTANDING OF MOE DESIGN CHOICES. In *ICLR 2024 Workshop on Mathematical and Empirical Understanding of Foundation Models*, 2024b. URL <https://openreview.net/forum?id=ebPKyb6r9F>.
- William Fedus, Barret Zoph, and Noam Shazeer. Switch transformers: Scaling to trillion parameter models with simple and efficient sparsity. *Journal of Machine Learning Research*, 23(120):1–39, 2022.
- Vlad Fomenko, Han Yu, Jongho Lee, Stanley Hsieh, and Weizhu Chen. A note on lora, 2024.
- Hélène A Gaspar and Matthew P Seddon. Glolloc: Mixture of global and local experts for molecular activity prediction. In *ICLR2022 Machine Learning for Drug Discovery*, 2022.
- Mandy Guo, Zihang Dai, Denny Vrandečić, and Rami Al-Rfou. Wiki-40b: Multilingual language model dataset. In *LREC 2020*, 2020. URL <http://www.lrec-conf.org/proceedings/lrec2020/pdf/2020.lrec-1.296.pdf>.
- Edward J Hu, Yelong Shen, Phillip Wallis, Zeyuan Allen-Zhu, Yuanzhi Li, Shean Wang, Lu Wang, and Weizhu Chen. Lora: Low-rank adaptation of large language models. *arXiv preprint arXiv:2106.09685*, 2021.
- Albert Q. Jiang, Alexandre Sablayrolles, Antoine Roux, Arthur Mensch, Blanche Savary, Chris Bamford, Devendra Singh Chaplot, Diego de las Casas, Emma Bou Hanna, Florian Bressand, Gianna Lengyel, Guillaume Bour, Guillaume Lample, Léo Renard Lavaud, Lucile Saulnier, Marie-Anne Lachaux, Pierre Stock, Sandeep Subramanian, Sophia Yang, Szymon Antoniak, Teven Le Scao, Théophile Gervet, Thibaut Lavril, Thomas Wang, Timothée Lacroix, and William El Sayed. Mixtral of experts, 2024.
- Damjan Kalajdzievski. A rank stabilization scaling factor for fine-tuning with lora, 2023.
- Brendan McMahan, Eider Moore, Daniel Ramage, Seth Hampson, and Blaise Agüera y Arcas. Communication-efficient learning of deep networks from decentralized data. In *Artificial intelligence and statistics*, pp. 1273–1282. PMLR, 2017.
- Amirkeivan Mohtashami, Florian Hartmann, Sian Gooding, Lukas Zilka, Matt Sharifi, et al. Social learning: Towards collaborative learning with large language models. *arXiv preprint arXiv:2312.11441*, 2023.
- OpenAI. URL [https://huggingface.co/docs/transformers/en/model\\_doc/gpt2](https://huggingface.co/docs/transformers/en/model_doc/gpt2).
- Sebastian Raschka. Practical tips for finetuning llms using lora (low-rank adaptation), 2023. URL <https://magazine.sebastianraschka.com/p/practical-tips-for-finetuning-llms>.

- 
- Daria Soboleva, Faisal Al-Khateeb, Robert Myers, Jacob R Steeves, Joel Hestness, and Nolan Dey. SlimPajama: A 627B token cleaned and deduplicated version of RedPajama. <https://www.cerebras.net/blog/slimpajama-a-627b-token-cleaned-and-deduplicated-version-of-redpajama>, 2023. URL <https://huggingface.co/datasets/cerebras/SlimPajama-627B>.
- Youbang Sun, Zitao Li, Yaliang Li, and Bolin Ding. Improving lora in privacy-preserving federated learning. *arXiv preprint arXiv:2403.12313*, 2024.
- Nicolas Wagner, Dongyang Fan, and Martin Jaggi. Personalized collaborative fine-tuning for on-device large language models. In *First Conference on Language Modeling*, 2024. URL <https://openreview.net/forum?id=bwo3GVsgOv>.
- Wikimedia-Foundation. Wikimedia downloads. URL <https://dumps.wikimedia.org>.
- Xun Wu, Shaohan Huang, and Furu Wei. Mixture of loRA experts. In *The Twelfth International Conference on Learning Representations*, 2024. URL <https://openreview.net/forum?id=uWvKBCYh4S>.
- Fuzhao Xue, Zian Zheng, Yao Fu, Jinjie Ni, Zangwei Zheng, Wangchunshu Zhou, and Yang You. Openmoe: An early effort on open mixture-of-experts language models, 2024.
- Liping Yi, Han Yu, Chao Ren, Heng Zhang, Gang Wang, Xiaoguang Liu, and Xiaoxiao Li. pFedmoe: Data-level personalization with mixture of experts for model-heterogeneous personalized federated learning, 2024.
- Ted Zadouri, Ahmet Üstün, Arash Ahmadian, Beyza Ermis, Acyr Locatelli, and Sara Hooker. Pushing mixture of experts to the limit: Extremely parameter efficient moe for instruction tuning. In *The Twelfth International Conference on Learning Representations*, 2024. URL <https://openreview.net/forum?id=EvDeiLv7qc>.
- Jianyi Zhang, Saeed Vahidian, Martin Kuo, Chunyuan Li, Ruiyi Zhang, Guoyin Wang, and Yiran Chen. Towards building the federated gpt: Federated instruction tuning. *arXiv preprint arXiv:2305.05644*, 2023.
- Xiang Zhang, Junbo Zhao, and Yann LeCun. Character-level convolutional networks for text classification, 2016.



## A LIMITATIONS AND SOCIETAL IMPACT

**Limitations.** Compared to FedAvg type of methods, our method requires extra gradient steps on routing parameters and memory storage for the routing parameters. Since a routing network is usually a one-layer MLP, the extra cost in computation and storage is relatively small.

The robust performance of our method relies on the fact that we update routing parameters and expert parameters on two independent losses. This means we need some validation samples independent from training samples. When local data size is minimal, this can be an issue.

Our method, while generally robust, still has a tendency towards overfitting when there is a significant mismatch between local resource abundance and data complexity, similar to other methods.

**Societal Impact.** We offer a collaboration framework for edge devices, aiming to enable smaller devices to leverage large language models (LLMs) despite limited resources and data availability. Our approach enhances fairness and mitigates privacy concerns by ensuring data remains on end devices. The privacy aspects can further be enhanced by differential privacy, which we do not pursue here.

The robustness towards attackers is beyond the scope of our work. Our collaboration framework has no guarantee of resilience towards Byzantine attackers, which could potentially lead to misuse by certain parties.

## B EXTRA EXPERIMENTAL DETAILS

Following Kalajdzievski (2023), we choose  $\gamma$  to be a rank-stabilized value, a technique which helps stabilize gradient norms.  $\alpha$  and the rank  $r$  are hyper-parameters to choose from. The LoRA modules function as follows:

$$W = W^0 + \gamma \cdot AB, \quad \gamma = \frac{\alpha}{\sqrt{r}} \quad (5)$$

All our experiments except the centralized ones were conducted on a single A100-SXM4-40GB GPU. The centralized learning baseline experiments were conducted on a single A100-SXM4-80GB GPU, as a batch size of 64\*4 requires a larger storage capacity.

For AG News and Multilingual Wikipedia data splits, we conduct 20 communication rounds. For SlimPajama data splits, due to greater category diversity, we conduct 50 communication rounds. Between each pair of communication rounds, there are 10 local iterations. In each iteration, a batch size of 64 is processed with a context length of 128. We set the routing update period to 30 iterations, and every time we update routing parameters, we do 10 gradient steps on the validation loss. The choice of the hyperparameters is from a sweep run and we provide the evidence in Figure 9.

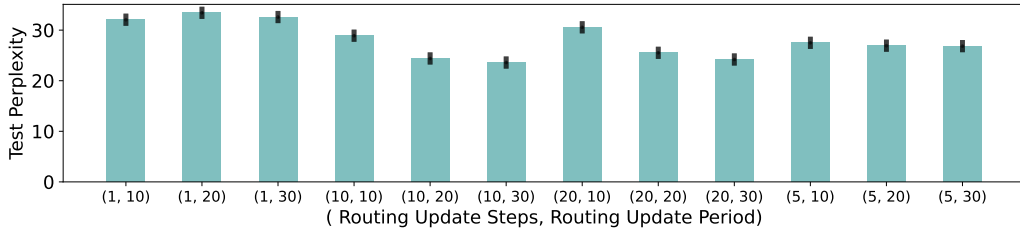


Figure 9: Sweep results on SlimPajama data splits. We ablate the impact of the update period ( $\tau$ ) and the number of update steps ( $s$ ) on model performance.

The number of tokens within each user is shown in Table 3.

|                     |            | user 0    | user 1    | user 2    | user 3    |
|---------------------|------------|-----------|-----------|-----------|-----------|
| <b>AG News</b>      | Training   | 761'924   | 756'719   | 814'131   | 771'460   |
|                     | Validation | 48'809    | 48'730    | 50'398    | 48'249    |
|                     | Test       | 48'167    | 47'721    | 48'344    | 49'377    |
| <b>Multilingual</b> | Training   | 557'662   | 407'498   | 556'796   | 451'584   |
|                     | Validation | 300'764   | 216'318   | 220'071   | 165'984   |
|                     | Test       | 229'720   | 219'741   | 210'570   | 172'547   |
| <b>SlimPajama</b>   | Training   | 1'000'000 | 1'000'000 | 1'000'000 | 1'000'000 |
|                     | Validation | 200'000   | 200'000   | 200'000   | 200'000   |
|                     | Test       | 200'000   | 200'000   | 200'000   | 200'000   |

Table 3: Number of tokens in each dataset splits

## C MORE TABLES AND FIGURES

### C.1 EXTENDED BASELINE COMPARISON

An extended version of Table 1 is presented in Table 4. In this extension, we incorporate two additional ablations: 1) Integration of a routing mechanism, updated simultaneously with the expert networks; 2) Iterative updates alternating between routing and expert parameters, with the routing parameters updated using newly-sampled training batches instead of a dedicated validation set. Moreover, we include another baseline method FFA-LoRA from Sun et al. (2024), where the LoRA A matrices are fixed at initialization.

Notably, the comparison between scenarios ii) and iii) reveals minimal disparity, underscoring the significance of having an independent validation set exclusively for routing parameter updates.





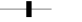































|   | AG News  | Multilingual  | SlimPajama  |
|---|--|---|---|
| i) Without routing  |  |   |   |
| <i>Pretrained</i>   | 90.65  | 156.12  | 37.19   |
| <i>Centralized</i>  | 28.19 (0.52)  | 55.41 (0.12)  | 19.53 (0.14)   |
| <i>Local</i>  | 41.50 (0.05)  | 55.49 (0.64)  | 27.31 (0.17)   |
| <i>FedAvg</i>   | 32.24 (0.05)  | 56.90 (0.16)  | 23.30 (0.17)   |
| <i>FFA-LoRA</i>   | 31.60 (0.14)  | 57.83 (0.13)  | 23.42 (0.069)  |
| <i>PCL</i>  | 32.11 (0.04)  | 54.02 (0.19)  | 27.12 (0.33)   |
| ii) Update routing and expert params simultaneously on training loss              |  |   |   |
| <i>Local-MoE</i>  | 41.38 (0.08)  | 55.78 (0.27)  | 27.35 (0.22)   |
| <i>FedAvg-MoE</i>   | 31.63 (0.07)  | 58.15 (0.10)  | 23.37 (0.12)   |
| iii) Alternating update routing params on newly sampled batches from training set |  |   |   |
| <i>Local-MoE - tr</i>   | NA   | 53.78 (0.33)  | 27.78 (0.06)   |
| <i>FedAvg-MoE - tr</i>  | NA   | 59.39 (0.13)  | 23.00 (0.01)   |
| <i>IGIS - tr</i>  | NA   | 50.86 (0.14)  | 25.45 (0.01)   |
| iv) Alternating update routing params on a validation set                         |  |   |   |
| <i>CoMiGS - 2S</i>  | 35.81 (0.13)  | 46.36 (0.16)  | 22.51 (0.08)   |
| <i>CoMiGS - 2G</i>  | 31.18 (0.05)  | 58.31 (0.17)  | 21.36 (0.01)   |
| <i>CoMiGS - IGIS</i>  | 33.53 (0.03)  | 47.19 (0.10)  | 21.79 (0.04)   |

Table 4: Mean test perplexity over users with homogenous models, averaged across 3 seeds. Mean (std) with a rank locator for the mean (the lower the better). Green denotes the best performing methods and red denotes our method.

|                     | No LB        | LB (uniform) | LB (generalist-favored) |
|---------------------|--------------|--------------|-------------------------|
| AG News (homo)      | 33.69 (0.21) | 33.53 (0.03) | 33.53 (0.03)            |
| AG News (hetero)    | 34.31 (0.05) | 34.28 (0.11) | 34.22 (0.09)            |
| Multi-Wiki (homo)   | 47.31 (0.15) | 47.19 (0.10) | 47.19 (0.10)            |
| Multi-Wiki (hetero) | 46.36 (0.16) | 46.15 (0.04) | 46.48 (0.16)            |
| SlimPajama (homo)   | 21.77 (0.02) | 21.79 (0.04) | 21.79 (0.04)            |
| SlimPajama (hetero) | 22.15 (0.07) | 22.10 (0.11) | 22.10 (0.17)            |

Table 5: Test perplexity with different load balancing terms with (hetero) or without (homo) system heterogeneity.

## C.2 HETLORA

Analogously to the baseline experiment comparison in FlexLoRA (Bai et al., 2024), we use  $\gamma = 0.99$  as pruning strength and sweep the regularization parameter in  $\{5 \times 10^{-2}, 5 \times 10^{-3}, 5 \times 10^{-4}\}$ .

## C.3 IS THE STANDARD LOAD BALANCING LOSS SUFFICIENT?

The standard load balancing loss encourages equal assignment of tokens to each expert. To encourage enough tokens to be routed to the generalist expert such that more general knowledge can be developed, we add a modified load-balancing loss to the outer optimization objective in eq equation 4 by introducing an **importance weighting**. We separate the 0-th expert to be the generalist expert and conduct Top-2 routing. The modified load balancing loss is as follows:

$$\mathcal{L}_i^{\text{LB}} = \frac{1}{(n_i - 1)^2 + 1} \cdot f_0 \cdot P_0 + \sum_{j=1}^{n_i-1} \frac{n_i - 1}{(n_i - 1)^2 + 1} \cdot f_j \cdot P_j \quad (6)$$

where

$$f_j = \frac{1}{T} \sum_{x \in \mathcal{B}} \mathbb{1}\{j \in \text{Top2 indices of } p(x)\} \quad P_j = \frac{1}{T} \sum_{x \in \mathcal{B}} p_j(x) \quad (7)$$

$j$  is the expert index and  $p(x) = [p_j(x)]_{j=1}^{n_i}$  is the logit output from the routing network for a specific token  $x$ . The idea is that one of the top 2 tokens should always be routed to the generalist expert, i.e. the 0-th expert. Thus,  $\frac{p_0}{1/2}$  should be equal to  $\frac{p_i}{1/2(n_i-1)}$  for  $i \neq 0$ . As the original load balancing loss encourages uniform distribution, this modification encourages the generalist expert to have a routing probability of 0.5 on expectation. Note that when  $n_i = 2$ , this  $\mathcal{L}_i^{\text{LB}}$  is the same as the original load balancing loss as proposed in Fedus et al. (2022).

We present the results in Table 5: in both scenarios, whether users have the same or different numbers of experts, including a load-balancing term leads to a slight improvement compared to omitting it. However, encouraging more tokens to be routed to the generalists does not make a significant difference.

## D ADDITIONAL EXPERIMENTS

We replicate the experiments in Section 4.3 with the SlimPajama dataset, where we assign four times as many tokens to Users 2 and 3 as to Users 0 and 1.

**More Specialists Help with Higher Data Quantity.** From Figure 10, it is clear that users 2 and 3 benefit from more experts locally.

**Generalists Help to Prevent Redundant Specialists from Over-Fitting?** From Figure 11, we observe more prominent overfitting than in Figure 7, likely because the tasks are objectively easier, as indicated by lower test perplexity from the beginning of fine-tuning. Generalists have limited power to prevent overfitting with easy tasks.

**Specialists Can Benefit Generalists.** Low-resourced users that can only support a single expert setup still benefit from collaboration, as the generalist knowledge is refined through a more detailed distinction between specialist and generalist roles via other high-resourced users.

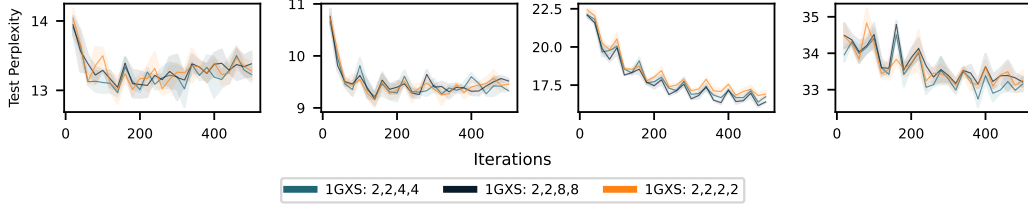


Figure 10: Test Perplexity during training for the SlimPajama setup. User 2 and User 3 have more local data and thus benefit from having more experts. The numbers in the legend indicate the number of experts  $n_i$  within each user. Top-2 routing is performed.

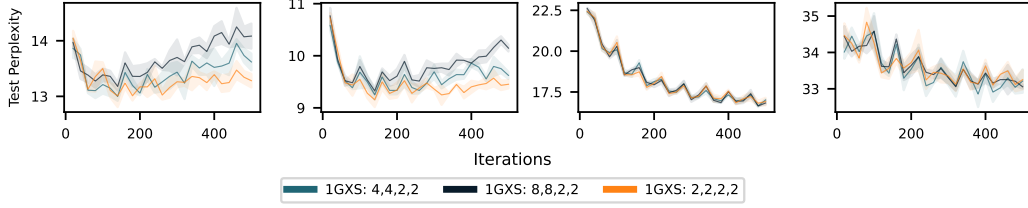


Figure 11: In this SlimPajama setup, Users 0 and 1 despite having low resources locally, overfit slightly on their small-sized local data. Numbers in the legend denote the number of experts  $n_i$  within each user. Top2 routing is performed.

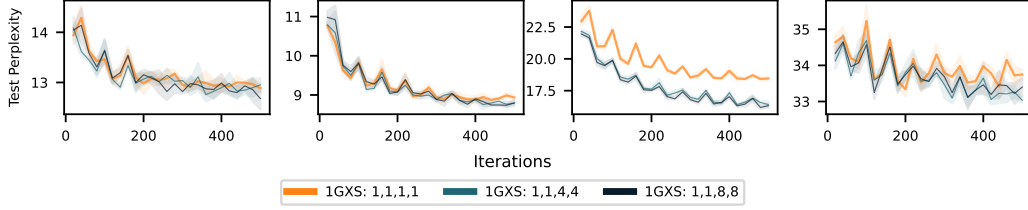


Figure 12: In this SlimPajama setup, Users 0 and 1, despite having only one expert locally, still benefit from other users having more experts, thereby enhancing the generalist’s performance. The numbers in the legend indicate the number of experts,  $n_i$ , within each user. Top-2 routing is applied when  $n_i \geq 2$

## E VISUALIZATION OF EXPERT SPECIALIZATION

To visualize which tokens are routed to the generalist and specialist experts for our *IGIS* model trained on SlimPajama, we ask ChatGPT to generate texts in the style of StackExchange, Python Codes, ArXiv Paper and Books. We then feed those texts to the user-specific models and color the token with the Top1 routed index. The routing results after the very first layer (0th), a middle layer (5th), and the very last layer (11th) are presented in Figure 13, 14 and 15.

We perform the same experiments on AG News, asking ChatGPT to generate News text on the topics World, Sports, Business, and Sci/Tech. The routing results after the very first layer (0th), a middle layer (5th), and the very last layer (11th) are presented in Figure 16, 17 and 18.

For all the plots, diagonal entries are *in-domain* texts and off-diagonal entries are *out-of-domain* texts.

|  |   |   |   |   |
|--|---|---|---|---|
| StackEx  | L1 and L2 regularization are techniques to prevent overfitting in machine learning models. L1 regularization (Lasso) adds the absolute value of the magnitude of coefficients as a penalty term to the loss function. This can result in sparse models with few coefficients, effectively performing feature selection. L2 regularization (Ridge) adds the squared magnitude of coefficients as a penalty term. This doesn't lead to sparse models but can prevent large coefficients.        | L1 and L2 regularization are techniques to prevent overfitting in machine learning models. L1 regularization (Lasso) adds the absolute value of the magnitude of coefficients as a penalty term to the loss function. This can result in sparse models with few coefficients, effectively performing feature selection. L2 regularization (Ridge) adds the squared magnitude of coefficients as a penalty term. This doesn't lead to sparse models but can prevent large coefficients.        | L1 and L2 regularization are techniques to prevent overfitting in machine learning models. L1 regularization (Lasso) adds the absolute value of the magnitude of coefficients as a penalty term to the loss function. This can result in sparse models with few coefficients, effectively performing feature selection. L2 regularization (Ridge) adds the squared magnitude of coefficients as a penalty term. This doesn't lead to sparse models but can prevent large coefficients.        | L1 and L2 regularization are techniques to prevent overfitting in machine learning models. L1 regularization (Lasso) adds the absolute value of the magnitude of coefficients as a penalty term to the loss function. This can result in sparse models with few coefficients, effectively performing feature selection. L2 regularization (Ridge) adds the squared magnitude of coefficients as a penalty term. This doesn't lead to sparse models but can prevent large coefficients.        |
|  | <pre>def fibonaccini(n):     fib = [0, 1]     for i in range(2, n):         fib.append(fib[-1] + fib[-2])     return fib print(fibonaccini(10))</pre>   | <pre>def fibonaccini(n):     fib = [0, 1]     for i in range(2, n):         fib.append(fib[-1] + fib[-2])     return fib print(fibonaccini(10))</pre>   | <pre>def fibonaccini(n):     fib = [0, 1]     for i in range(2, n):         fib.append(fib[-1] + fib[-2])     return fib print(fibonaccini(10))</pre>   | <pre>def fibonaccini(n):     fib = [0, 1]     for i in range(2, n):         fib.append(fib[-1] + fib[-2])     return fib print(fibonaccini(10))</pre>   |
|  | We present novel quantum algorithms that significantly improve the efficiency of solving linear systems of equations. Our approach leverages quantum phase estimation and amplitude amplification to achieve an exponential speed up over classical counterparts. We demonstrate that our algorithms can solve $\ Ax = b\ $ with complexity $\mathcal{O}(\log(N))$ , where $N$ is the dimension of the system, under specific conditions. Numerical simulations confirm the robustness of our | We present novel quantum algorithms that significantly improve the efficiency of solving linear systems of equations. Our approach leverages quantum phase estimation and amplitude amplification to achieve an exponential speed up over classical counterparts. We demonstrate that our algorithms can solve $\ Ax = b\ $ with complexity $\mathcal{O}(\log(N))$ , where $N$ is the dimension of the system, under specific conditions. Numerical simulations confirm the robustness of our | We present novel quantum algorithms that significantly improve the efficiency of solving linear systems of equations. Our approach leverages quantum phase estimation and amplitude amplification to achieve an exponential speed up over classical counterparts. We demonstrate that our algorithms can solve $\ Ax = b\ $ with complexity $\mathcal{O}(\log(N))$ , where $N$ is the dimension of the system, under specific conditions. Numerical simulations confirm the robustness of our | We present novel quantum algorithms that significantly improve the efficiency of solving linear systems of equations. Our approach leverages quantum phase estimation and amplitude amplification to achieve an exponential speed up over classical counterparts. We demonstrate that our algorithms can solve $\ Ax = b\ $ with complexity $\mathcal{O}(\log(N))$ , where $N$ is the dimension of the system, under specific conditions. Numerical simulations confirm the robustness of our |
|  | In the quiet village of Eldoria, nestled between rolling hills and ancient forests, lived a young girl named Elara. She possessed a curious mind and an adventurous spirit, always yearning to explore beyond the familiar paths. One fateful day, while wandering through the woods, she discovered a hidden glen bathed in golden light. In the center stood an ancient oak tree, its branches stretching towards the heavens. As Elara approached, she noticed a shimmering                | In the quiet village of Eldoria, nestled between rolling hills and ancient forests, lived a young girl named Elara. She possessed a curious mind and an adventurous spirit, always yearning to explore beyond the familiar paths. One fateful day, while wandering through the woods, she discovered a hidden glen bathed in golden light. In the center stood an ancient oak tree, its branches stretching towards the heavens. As Elara approached, she noticed a shimmering                | In the quiet village of Eldoria, nestled between rolling hills and ancient forests, lived a young girl named Elara. She possessed a curious mind and an adventurous spirit, always yearning to explore beyond the familiar paths. One fateful day, while wandering through the woods, she discovered a hidden glen bathed in golden light. In the center stood an ancient oak tree, its branches stretching towards the heavens. As Elara approached, she noticed a shimmering                | In the quiet village of Eldoria, nestled between rolling hills and ancient forests, lived a young girl named Elara. She possessed a curious mind and an adventurous spirit, always yearning to explore beyond the familiar paths. One fateful day, while wandering through the woods, she discovered a hidden glen bathed in golden light. In the center stood an ancient oak tree, its branches stretching towards the heavens. As Elara approached, she noticed a shimmering                |
| User 0                      User 1                      User 2                      User 3 |   |   |   |   |

Figure 13: Visualization of token-level routing results for *IGIS* trained on SlimPajama. Tokens are colored with the first expert choice at the 0th (first) layer. Orange denotes the generalist and blue denotes the specialist. Users 0-3 are trained on the categories StackExchange, GitHub, ArXiv, and Book respectively. Texts are generated by ChatGPT.

|         |   |   |   |   |
|---------|---|---|---|---|
| StackEx | L1 and L2 regularization are techniques to prevent overfitting in machine learning models. L1 regularization (Lasso) adds the absolute value of the magnitude of coefficients as a penalty term to the loss function. This can result in sparse models with few coefficients, effectively performing feature selection. L2 regularization (Ridge) adds the squared magnitude of coefficients as a penalty term. This doesn't lead to sparse models but can prevent large coefficients.        | L1 and L2 regularization are techniques to prevent overfitting in machine learning models. L1 regularization (Lasso) adds the absolute value of the magnitude of coefficients as a penalty term to the loss function. This can result in sparse models with few coefficients, effectively performing feature selection. L2 regularization (Ridge) adds the squared magnitude of coefficients as a penalty term. This doesn't lead to sparse models but can prevent large coefficients.        | L1 and L2 regularization are techniques to prevent overfitting in machine learning models. L1 regularization (Lasso) adds the absolute value of the magnitude of coefficients as a penalty term to the loss function. This can result in sparse models with few coefficients, effectively performing feature selection. L2 regularization (Ridge) adds the squared magnitude of coefficients as a penalty term. This doesn't lead to sparse models but can prevent large coefficients.        | L1 and L2 regularization are techniques to prevent overfitting in machine learning models. L1 regularization (Lasso) adds the absolute value of the magnitude of coefficients as a penalty term to the loss function. This can result in sparse models with few coefficients, effectively performing feature selection. L2 regularization (Ridge) adds the squared magnitude of coefficients as a penalty term. This doesn't lead to sparse models but can prevent large coefficients.        |
|         | <pre>def fibonaccini(n):     fib = [0, 1]     for i in range(2, n):         fib.append(fib[-1] + fib[-2])     return fib print(fibonaccini(10))</pre>   | <pre>def fibonaccini(n):     fib = [0, 1]     for i in range(2, n):         fib.append(fib[-1] + fib[-2])     return fib print(fibonaccini(10))</pre>   | <pre>def fibonaccini(n):     fib = [0, 1]     for i in range(2, n):         fib.append(fib[-1] + fib[-2])     return fib print(fibonaccini(10))</pre>   | <pre>def fibonaccini(n):     fib = [0, 1]     for i in range(2, n):         fib.append(fib[-1] + fib[-2])     return fib print(fibonaccini(10))</pre>   |
|         | We present novel quantum algorithms that significantly improve the efficiency of solving linear systems of equations. Our approach leverages quantum phase estimation and amplitude amplification to achieve an exponential speed up over classical counterparts. We demonstrate that our algorithms can solve $\ Ax = b\ $ with complexity $\mathcal{O}(\log(N))$ , where $N$ is the dimension of the system, under specific conditions. Numerical simulations confirm the robustness of our | We present novel quantum algorithms that significantly improve the efficiency of solving linear systems of equations. Our approach leverages quantum phase estimation and amplitude amplification to achieve an exponential speed up over classical counterparts. We demonstrate that our algorithms can solve $\ Ax = b\ $ with complexity $\mathcal{O}(\log(N))$ , where $N$ is the dimension of the system, under specific conditions. Numerical simulations confirm the robustness of our | We present novel quantum algorithms that significantly improve the efficiency of solving linear systems of equations. Our approach leverages quantum phase estimation and amplitude amplification to achieve an exponential speed up over classical counterparts. We demonstrate that our algorithms can solve $\ Ax = b\ $ with complexity $\mathcal{O}(\log(N))$ , where $N$ is the dimension of the system, under specific conditions. Numerical simulations confirm the robustness of our | We present novel quantum algorithms that significantly improve the efficiency of solving linear systems of equations. Our approach leverages quantum phase estimation and amplitude amplification to achieve an exponential speed up over classical counterparts. We demonstrate that our algorithms can solve $\ Ax = b\ $ with complexity $\mathcal{O}(\log(N))$ , where $N$ is the dimension of the system, under specific conditions. Numerical simulations confirm the robustness of our |
|         | In the quiet village of Eldoria, nestled between rolling hills and ancient forests, lived a young girl named Elara. She possessed a curious mind and an adventurous spirit, always yearning to explore beyond the familiar paths. One fateful day, while wandering through the woods, she discovered a hidden glen bathed in golden light. In the center stood an ancient oak tree, its branches stretching towards the heavens. As Elara approached, she noticed a shimmering                | In the quiet village of Eldoria, nestled between rolling hills and ancient forests, lived a young girl named Elara. She possessed a curious mind and an adventurous spirit, always yearning to explore beyond the familiar paths. One fateful day, while wandering through the woods, she discovered a hidden glen bathed in golden light. In the center stood an ancient oak tree, its branches stretching towards the heavens. As Elara approached, she noticed a shimmering                | In the quiet village of Eldoria, nestled between rolling hills and ancient forests, lived a young girl named Elara. She possessed a curious mind and an adventurous spirit, always yearning to explore beyond the familiar paths. One fateful day, while wandering through the woods, she discovered a hidden glen bathed in golden light. In the center stood an ancient oak tree, its branches stretching towards the heavens. As Elara approached, she noticed a shimmering                | In the quiet village of Eldoria, nestled between rolling hills and ancient forests, lived a young girl named Elara. She possessed a curious mind and an adventurous spirit, always yearning to explore beyond the familiar paths. One fateful day, while wandering through the woods, she discovered a hidden glen bathed in golden light. In the center stood an ancient oak tree, its branches stretching towards the heavens. As Elara approached, she noticed a shimmering                |
|         | User 0  | User 1  | User 2  | User 3  |

Figure 14: Visualization of token-level routing results for *IGIS* trained on SlimPajama. Tokens are colored with the first expert choice at the 5th layer. Orange denotes the generalist and blue denotes the specialist. Users 0-3 are trained on the categories StackExchange, GitHub, ArXiv, and Book respectively. Texts are generated by ChatGPT.



Figure 15: Visualization of token-level routing results for *IGIS* trained on SlimPajama. Tokens are colored with the first expert choice at the 11th (last) layer. Orange denotes the generalist and blue denotes the specialist. Users 0-3 are trained on the categories StackExchange, GitHub, ArXiv, and Book respectively. Texts are generated by ChatGPT.





Figure 16: Visualization of token-level routing results for *IGIS* trained on AG News. Tokens are colored with the first expert choice at the 0th (first) layer. **Orange** denotes the generalist and **blue** denotes the specialist. Users 0-3 are with training data from AG News categories World, Sports, Business, and Sci/Tech respectively. Texts are generated by ChatGPT.





Figure 17: Visualization of token-level routing results for *IGIS* trained on AG News. Tokens are colored with the first expert choice at the 5th (middle) layer. Orange denotes the generalist and blue denotes the specialist. Users 0-3 are with training data from AG News categories World, Sports, Business, and Sci/Tech respectively. Texts are generated by ChatGPT.



Figure 18: Visualization of token-level routing results for *IGIS* trained on AG News. Tokens are colored with the first expert choice at the 11th (last) layer. Orange denotes the generalist and blue denotes the specialist. Users 0-3 are with training data from AG News categories World, Sports, Business, and Sci/Tech respectively. Texts are generated by ChatGPT.